

2023

Section: Chemistry

Novel Technique In Production Of Pb (II)- Imprinted Polymers

Ehab Mohammed

Department of chemistry, Faculty of science, Al-Azhar university, Nasr city, Egypt, xfahd88@yahoo.com

Mostafa M. Elsheikh

Ph.D. in organic chemistry, Faculty of Science, Ain Shams University, Cairo, Egypt.

Adham A. El-Zomrawy

Department of chemistry, Faculty of science, Al-Azhar university, Nasr city, Egypt

Farag A. Ahmed

Department of chemistry, Faculty of science, Al-Azhar university, Nasr city, Egypt

Follow this and additional works at: <https://absb.researchcommons.org/journal>

 Part of the [Physical Chemistry Commons](#), and the [Polymer Chemistry Commons](#)

How to Cite This Article

Mohammed, Ehab; Elsheikh, Mostafa M.; El-Zomrawy, Adham A.; and Ahmed, Farag A. (2023) "Novel Technique In Production Of Pb (II)- Imprinted Polymers," *Al-Azhar Bulletin of Science*: Vol. 34: Iss. 1, Article 5.

DOI: <https://doi.org/10.58675/2636-3305.1633>

This Original Article is brought to you for free and open access by Al-Azhar Bulletin of Science. It has been accepted for inclusion in Al-Azhar Bulletin of Science by an authorized editor of Al-Azhar Bulletin of Science. For more information, please contact kh_Mekheimer@azhar.edu.eg.

Novel Technique in Production of Pb (II)- Imprinted Polymers

Ehab Ramadan Mohammed ^{a,*}, Mostafa Mohammed Elsheikh ^b,
Adham Abdulsalam El-Zomrawy ^c, Farag Abdul Hai Ahmed ^d

^a Department of Special Chemistry, Faculty of Science, Al-Azhar University, Cairo, Egypt

^b Department of Organic Chemistry, Faculty of Science, Ain Shams University, Cairo, Egypt

^c Department of Physical Chemistry, Faculty of Science, Al-Azhar University, Cairo, Egypt

^d Department of Applied Chemistry, Faculty of Science, Al-Azhar University, Cairo, Egypt

Abstract

Ion imprinting techniques were used to produce ion imprinted polymer (IIP) particles for the selective removal of Pb^{2+} from aqueous environments. As the Templating monomers, acrylic acid, acrylic amine ligand, and Methylene Bisacrylamide crosslinker were chosen. The imprinted polymer was prepared by free radical polymerization. By leaching with 0.1 M HCl, the (Pb^{2+}) ion was removed from the template. The polymer particles were characterized by IR spectroscopy, Thermal analysis and potentiometric analysis. The produced polymer was mechanically crushed into fine particles, assembled into a sensor probe, and linked to a bare HB graphite pencil electrode (GPE). The sensor has a linear dynamic range for Lead (II) ion determination of 4.5–50 ppb and provides best results at pH 4.6 under conditions of continual stirring. In a setting with many analytes, the sensor has been applied to monitor Lead (II) ions. The prepared samples showed high thermal stability with high selectivity for electrochemical detection of lead metal ions.

Keywords: Acrylic polymers, Free radical polymerization, Ion imprinted polymers, Lead ion, Toxic heavy metals

1. Introduction

It is urgently necessary to develop both treatment and detection approaches in an industrial society due to contamination with very hazardous heavy metals that have very low toxicity limits. The environmental effects of these pollutants have catastrophic consequences for living organisms and plants. Therefore, accurate and specific detection of these ions is crucial to health Wu and colleagues [1].

Atomic absorption spectrometry (AAS), inductively coupled plasma atomic emission spectrometric (ICP-AES), and solid phase spectrophotometry (SPS) are a few of the methods used to evaluate contaminants Lu and colleagues [2]. Anodic stripping voltammetry (ASV) is the most widely used method for detecting and determining the existence of heavy metals in aqueous solutions. This method uses a square wave and a differential pulse anodic stripping voltammetry

(DPASV) Marton and colleagues, Zhai and colleagues [3–8], to realize the redissolution step square wave anodic stripping voltammetric (SWASV) Sylvestre and colleagues, Khadro and colleagues [9–11].

Sensors made by MIP technique is one of the most recent technologies for applying in ASV testing method for detection of Pb^{2+} as one of the most harmful heavy metals.

Imprinted polymerization is a process that turns monomers into imprinted polymers that are selective for the target analyte when polymerized in a solution containing the particular analyte Hasanah and colleagues [12].

The process of ion imprinted polymer (IIP) elaboration in the following three steps (1) metal ion complexation with a suitable ligand (2) Polymerization of the generated complex with a cross linker (3) the template ion is eliminated after polymerization Deng and colleagues [13]. The properties of IIPs are

Received 16 November 2022; revised 14 December 2022; accepted 14 December 2022.
Available online 3 October 2023

* Corresponding author. Bani Hani / u young / m center, Ahnasia city, 62734, Egypt.
E-mail address: xfahd88@yahoo.com (E.R. Mohammed).

<https://doi.org/10.21608/2636-3305.1633>

2636-3305/© 2023, The Authors. Published by Al-Azhar university, Faculty of science. This is an open access article under the CC BY-NC-ND 4.0 Licence (<https://creativecommons.org/licenses/by-nc-nd/4.0/>).

Table 1. Experiments of group (1) that contain the ligand monomer.

Experiment	Acrylic acid [mmol]	Ligand [mmol]	Metal Ion [mmol]	Crosslinker [mmol]	Initiator [mmol]
Exp 1	15	10	5	40	1
Exp 2	15	10	5	50	0.8

Table 2. Experiments of group (2) that doesn't contain the ligand monomer.

Experiment	Acrylic acid [mmol]	Metal ion [mmol]	Crosslinker [mmol]	Initiator [mmol]
Exp 3	15	5	40	1
Exp 4	15	5	50	0.8

exceptional due to their extreme selectivity due to the memory effect from the preparation method. This high selectivity is mainly due to the Size and form of the produced cavities and the ligand's compatibility with the target ion Fereidoonipour and Rajabi [14]. As recognition sites are generated by certain ligands self-assembling around the metal ion and then cross-linking, this configuration allows the binding sites to match the charge, size, and coordination number of the ion Ventura and colleagues [15]. Additionally, the crosslinking and leaching processes can preserve the complicated geometry, creating a favourable environment for the template ion rebinding. IIPs can be thought of as artificial affinity media for these reasons

Deng and colleagues [13]. So, the scope of this study is how to find a methodology for production of Pb (II) imprinted polymers for using it as indicators for heavy harmful Pb (II) for industrial usage.

2. Experimental

2.1. Materials

Lead (II) oxide (PbO) was obtained from Loba-chem, India, acrylic acid (AA) was purchased from Arkema., France, N, N'-methylene bis(acrylamide) (MBA) was purchased from Sisco Research Laboratories (SRL) - India, 2-(Dimethylamino) ethyl methacrylate and 2, 2'-Azobis [2-(2-imidazolin-2-yl) propane] dihydrochloride (VA-044) were purchased from Sigma Aldrich (USA), Distilled and deionized water were used throughout the experiments.

2.2. Methodology

2.2.1. Preparation of Pb (II) imprinted polymer

The Pb²⁺ imprinted polymer was prepared by free radical polymerization, PbO was dissolved in deionized water, acrylic acid was added and Shaked thoroughly until complete solubilization followed by 2-Dimethylamino ethyl methacrylate as a ligand and N, N'-Methylene bisacrylamide (MBA) as a cross-linker. After that, 2, 2'-Azobis [2-(2-imidazolin-2-yl)

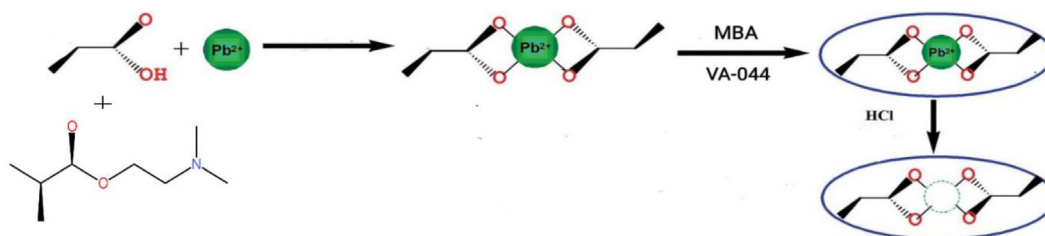
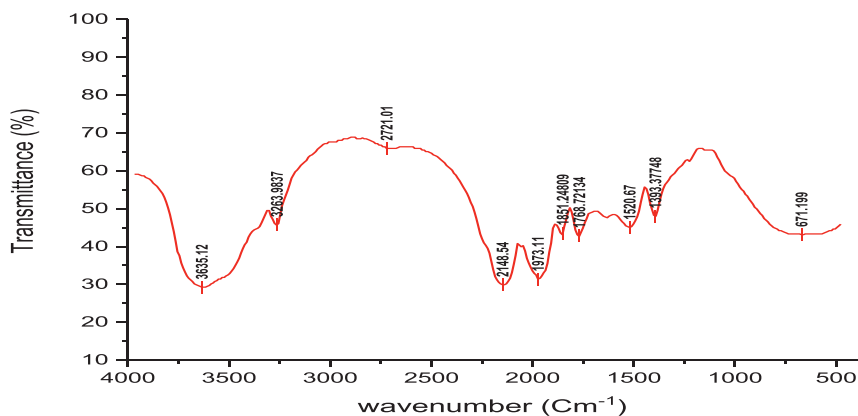
Fig. 1. Schematic representation of an Pb²⁺ IP synthesis.

Fig. 2. FT-IR spectra of exp (1).

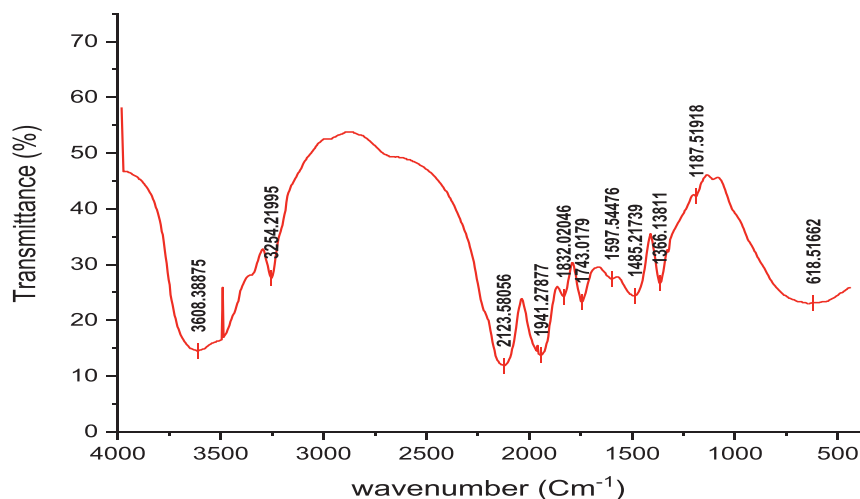


Fig. 3. FT-IR spectra of exp (2).

Table 3. TGA records for group (1).

Experiment	First stage %	Second stage %	Mass fraction of total weight loss (%) at 900 °C	Char Residue % at 900 °C
Exp (1)	19.08	52.57	71.6	28.4
Exp (2)	19.1	56.19	75.29	24.71

propane] dihydrochloride (VA-044) [water soluble initiator] was added.

The mixture was vigorously shaken after every addition of ingredients. Polymerization process was carried out for 24 h in a thermostat water bath at 60–70 °C with constant stirring. The produced imprinted polymer was twice or three times washed with deionized water to remove unreacted monomer, dried well, and then crushed, powdered, and sieved before being stored.

To leach the ion from the IIP template, IIP samples were treated with 0.1 M HCl. This procedure was repeated 3 times to ensure the absence of the template (Pb^{2+}).

Experiments were divided into two groups. The first group includes the prepared samples in presence of the ligand monomer and the second group does not contain the ligand monomer to study the effect of its presence and absence on the selectivity of the prepared polymer according to the following Tables 1 and 2, Fig. 1.

2.3. Characterization of polymers

2.3.1. FTIR spectrophotometer

Fourier transform infrared (FTIR) spectra of imprinted polymers were measured using a

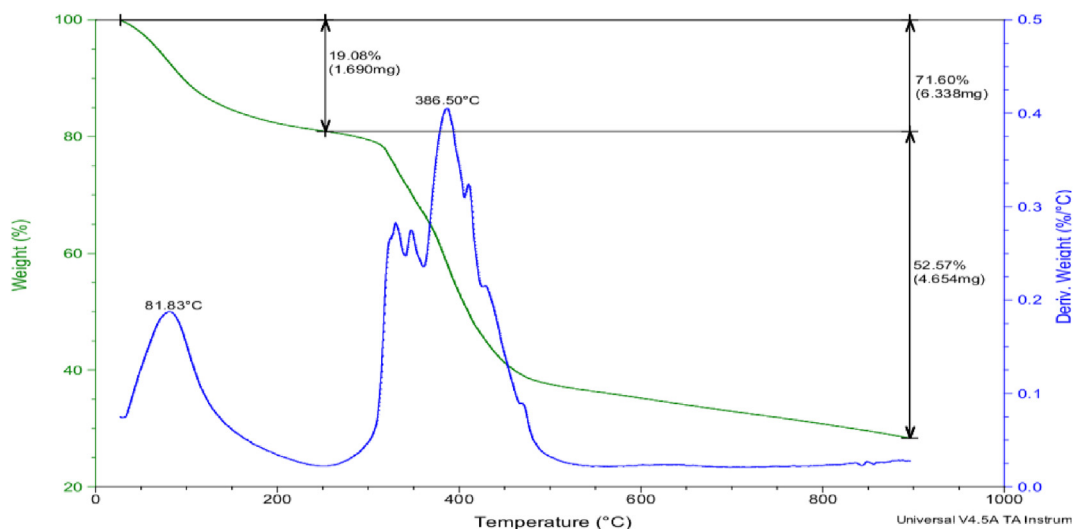


Fig. 4. TGA thermograms of exp (1).

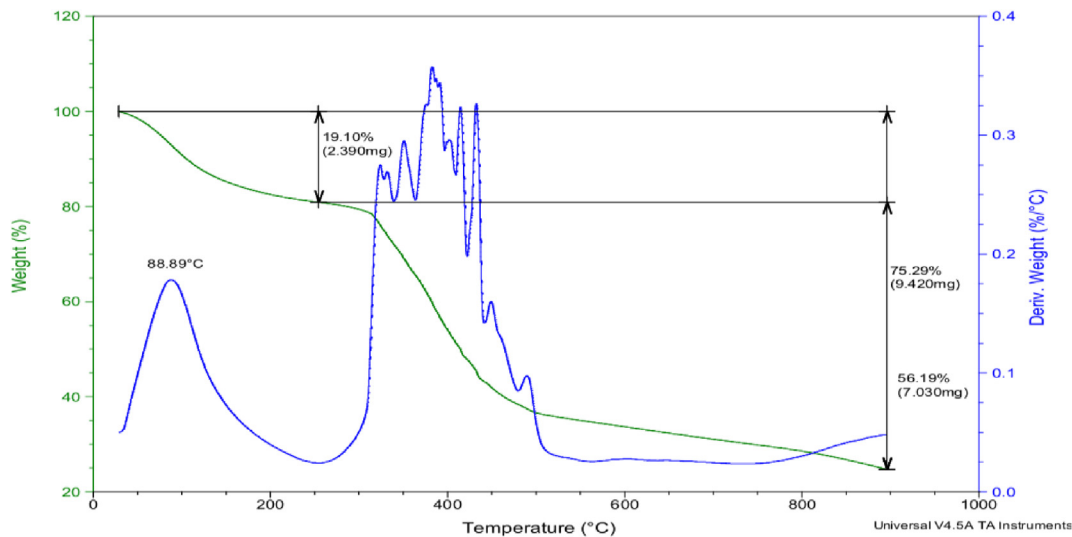


Fig. 5. TGA thermograms of exp (2).

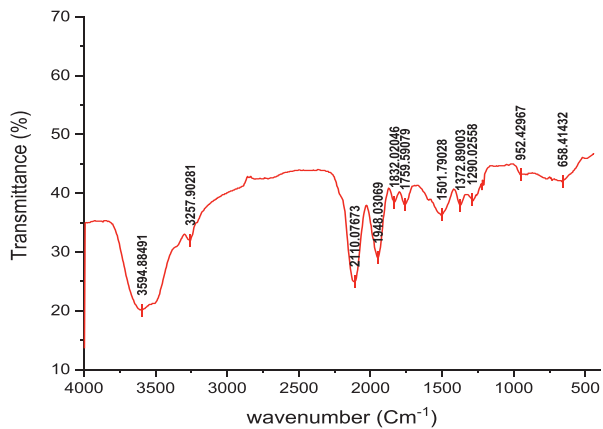


Fig. 6. FT-IR spectra of exp (3).

Table 4. TGA records for group (2).

Experiment	First stage %	Second stage %	Mass fraction of total weight loss (%) at 900 °C	Char Residue (%) at 900 °C
Exp (3)	17.38	62.33	79.71	20.29
Exp (4)	18.93	75.99	94.92	5.08

(Thermo Nicolet Avatar370) spectrometer and the KBr pellet technique in the 4000-500 cm^{-1} range at room temperature.

2.3.2. Thermal gravimetric analysis (TGA)

TGA Q500, (TA instruments) was used to evaluate the thermal stabilities of the films, thermo balance

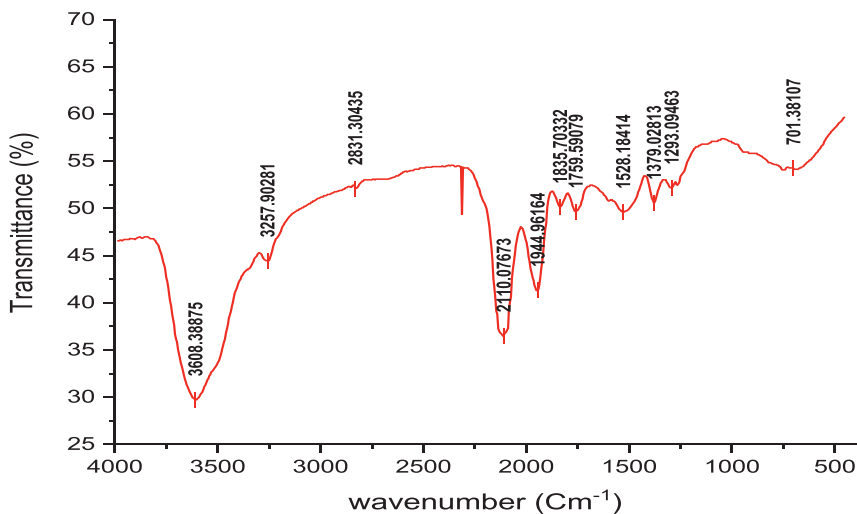


Fig. 7. FT-IR spectra of exp (1).

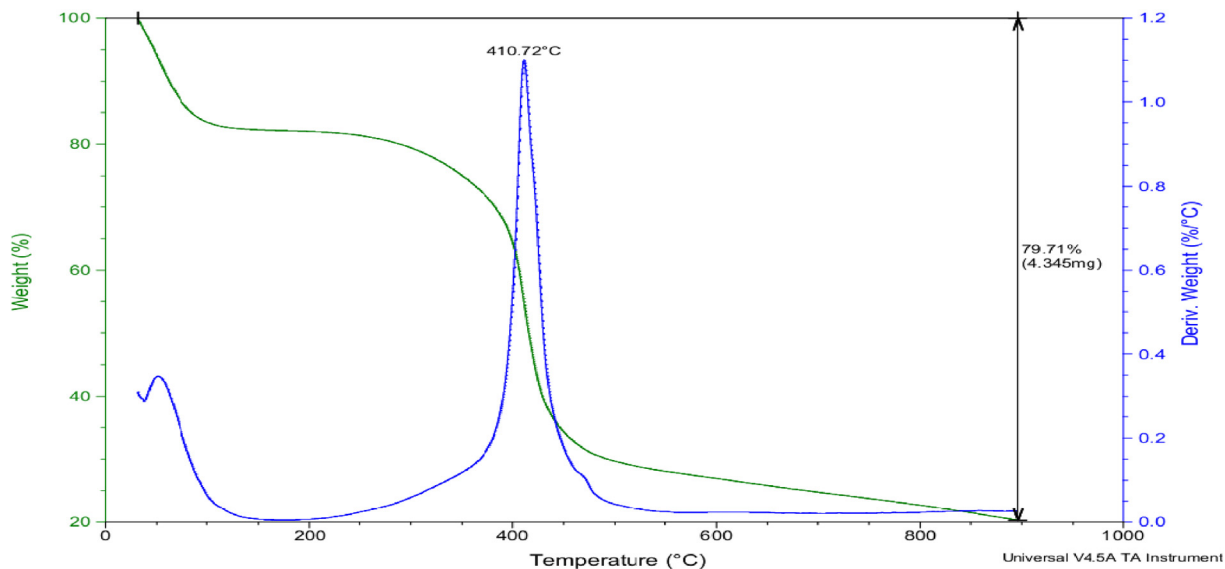


Fig. 8. TGA thermograms of exp (3).

sensitivity $0.1\mu\text{g}$. Samples were heated in nitrogen, flowing rate at 50 ml min^{-1} from 25 to $500\text{ }^{\circ}\text{C}$ at a heating rate of $10\text{ }^{\circ}\text{C min}^{-1}$. Sample weights ranging from 5 mg to 10 mg were used.

2.3.3. Electrochemical analysis

Cyclic voltammetry (CV), and square wave voltammetry (SWV) were measured using a Gamry Reference 3000 electrochemical workstation with a standard three-electrode system. A bare or modified graphite pencil electrode (GPE) was the working electrode, An Ag/AgCl electrode and a platinum

wire were adopted as the reference and counter electrodes, respectively.

3. Results and discussion

3.1. Characterization of group (1)

3.1.1. FTIR spectroscopy

Figure 2 shows that there are no bands in the range of $1638\text{--}1648\text{ cm}^{-1}$ and this is clear evidence that there are no vinyl groups in the polymer particles. This result might be explained by the complete polymerization of

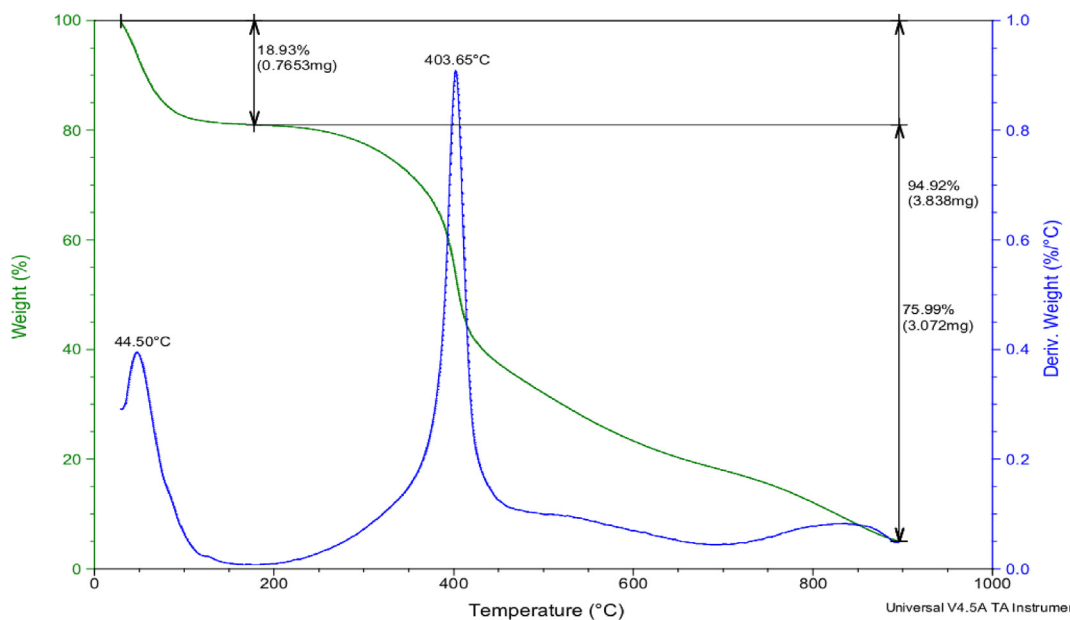


Fig. 9. TGA thermograms of exp (4).

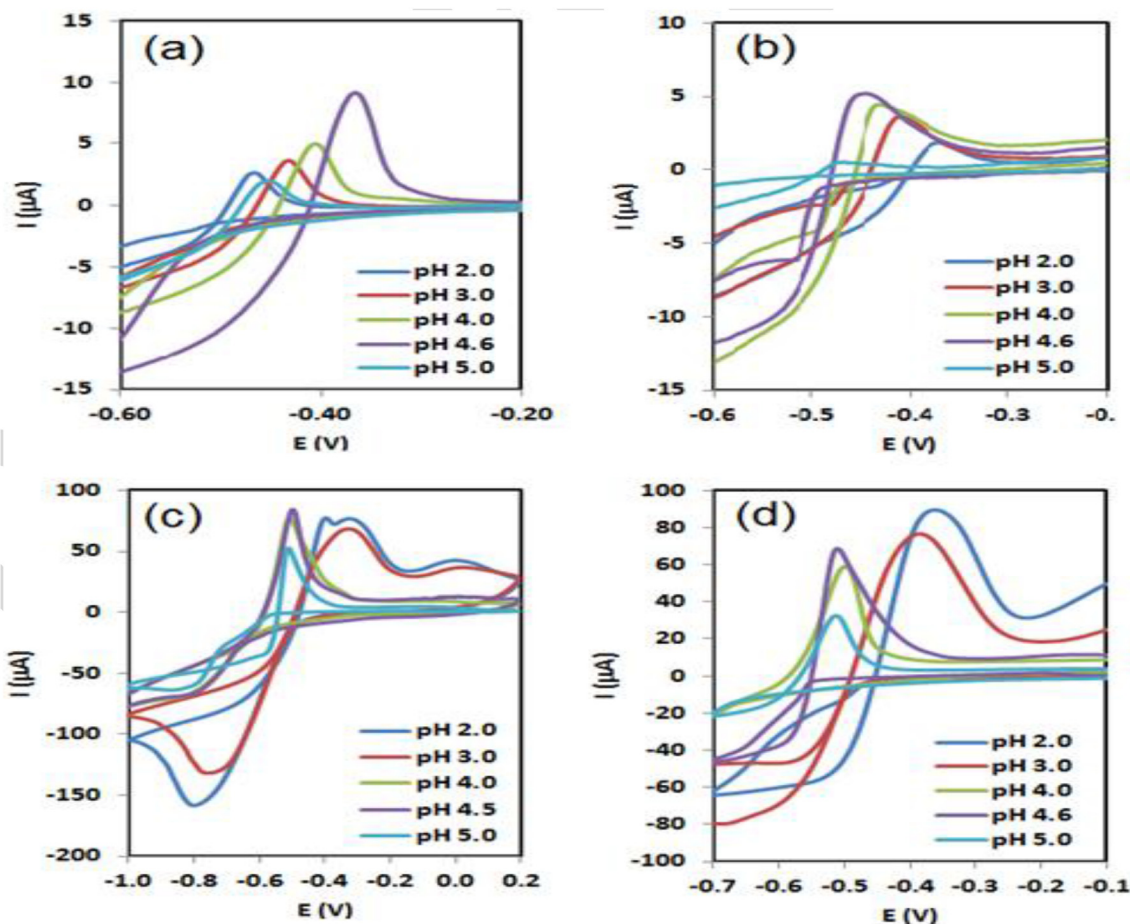


Fig. 10. Cyclic voltammograms curves of the exp 1/GPE (a), exp 2/GPE (b), exp 3/GPE (c), exp 4/GPE (d), for the individual analysis of Pb (II) ions at various pH values.

the prepared polymers, including DMAEMA, AA, and MBA. The band 3635.12 could indicate the presence O–H group of excess AA, 3263.9837 indicates the presence N–H group of excess MBA while the bands 1768.72134, 1851.24 indicates the presence C=O group which belongs to AA and MBA, respectively.

Figure 3 shows that there are no bands in the range of 1638–1648 cm^{-1} and this is clear evidence that there are no vinyl groups in the polymer particles. This result might be explained by the complete polymerization of the prepared polymers, including DMAEMA, AA, and MBA. The band 3608.38875 could indicate the presence O–H group of excess AA, 3254.21995 indicates the presence N–H group of excess MBA while the bands 1743.0179, 1832.02046 indicates the presence C=O group which belongs to AA and MBA, respectively.

3.1.2. Thermal gravimetric analysis

The thermal stabilities of AA – DMAEMA copolymer crosslinked by MBA were performed by TGA technique and the data obtained from the curves analysis in Table 3 and thermo-grams shown in Figs. 4

and 5. It is clear that the polymer samples exp (1) and exp (2) showed high thermal stability from room temperature to 900 °C. The thermogram showed two stages of thermal decomposition. The first stage from room temperature to 400 °C with a maximum at 250 °C exhibits a weight loss of 19.08% may be due to the removal of residual monomers and trapped water molecules. The second stage from 400 to 900 °C This decomposition is characterized by a weight loss of 52.57% due to short chain fragments created by chain scission. However, the differences between the two polymers in weight loss in the two stages during the analysis is not markable, polymer of exp (1) can be considered little more thermally stable than polymer of exp (2).

3.2. Characterization of group (2)

3.2.1. FTIR spectroscopy

Figure 6 shows that there are no bands in the range of 1638–1648 cm^{-1} and this is clear evidence

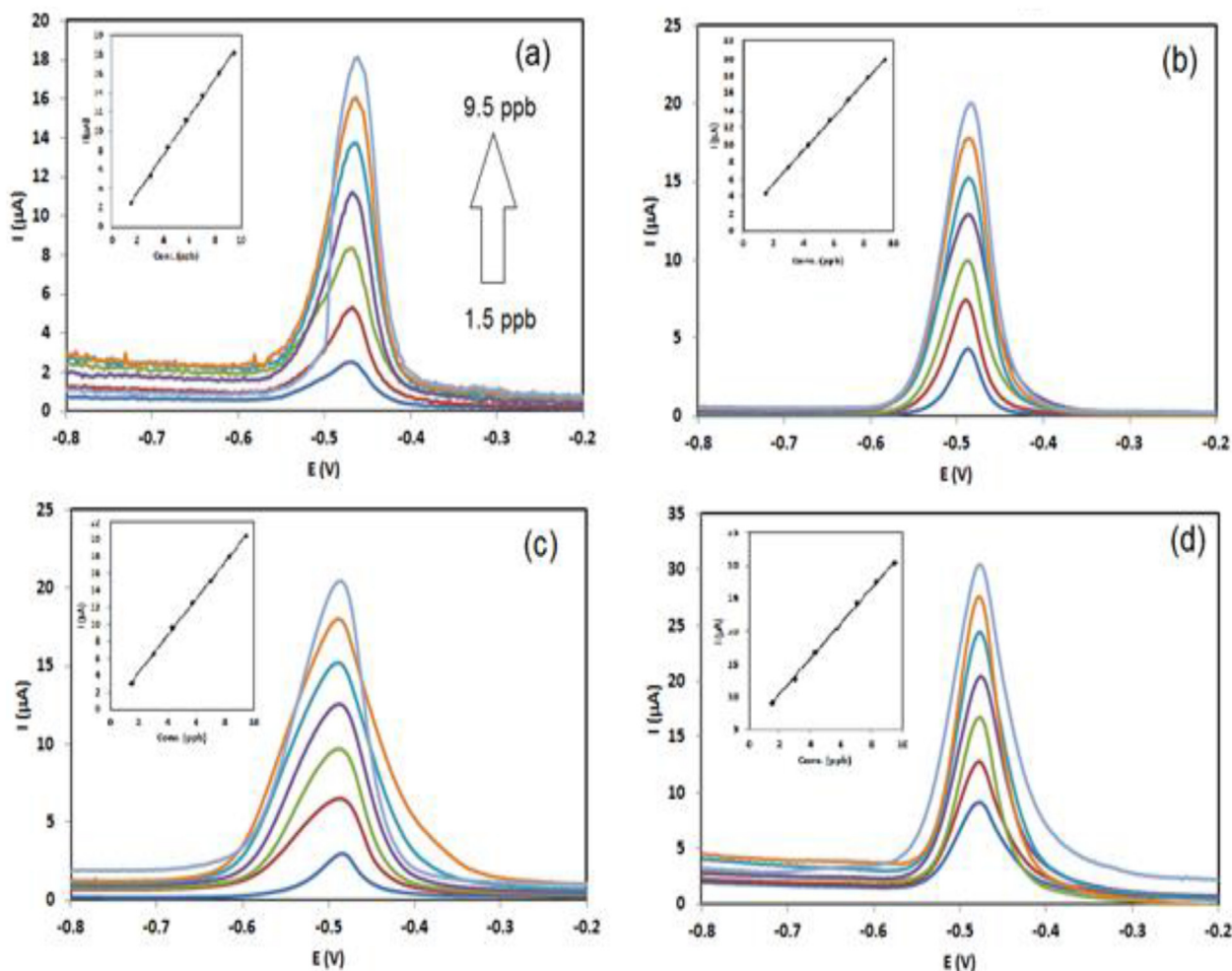


Fig. 11. SWV responses of the exp 1/GPE (a), exp 2/GPE (b), exp 3/GPE (c), exp 4/GPE (d), for the individual analysis of Pb (II) ions. (Insets were the corresponding calibration plots of stripping peak current against concentrations).

that there are no vinyl groups in the polymer particles. This result might be explained by the complete polymerization of the prepared polymers, including AA, and MBA. The band 3594.88491 could indicate the presence O–H group of excess AA, 3257.90281 indicates the presence N–H group of excess MBA while the bands 1759.59079, 1832.02046 indicates the presence C=O group which belongs to AA and MBA, respectively.

Figure 7 shows that there are no bands in the range of 1638–1648 cm^{-1} and this is clear evidence

that there are no vinyl groups in the polymer particles. This result might be explained by the complete polymerization of the prepared polymers, including DMAEMA, AA, and MBA. The band 3608.38875 could indicate the presence O–H group of excess AA, 3257.90281 indicates the presence N–H group of excess MBA while the bands 1759.59079, 1835.70332 indicates the presence C=O group which belongs to AA and MBA, respectively.

3.2.2. Thermal gravimetric analysis

Thermo-gravimetric analysis of group (2) was also investigated using TGA analysis. The data obtained from the curves analysis in Table 4 and thermograms shown in Figs. 8 and 9. The two polymers showed good thermal stability from room temperature to 900 °C.

The thermogram of exp (3) showed two stages of thermal decomposition. The first stage from room temperature to 400 °C with a maximum at 250 °C

Table 5. The corresponding constants and correlation coefficient for linear equation of experiments of group (1) and group (2).

Modified Electrode	A	b ($\mu\text{A ppb}^{-1}$)	R ²
Exp 1/GPE	0.3452	1.979	0.9982
Exp 2/GPE	1.5248	1.962	0.9996
Exp 3/GPE	0.0305	2.170	0.9989
Exp 4/GPE	5.0064	2.710	0.9989

Table 6. Comparison of Pb (II) sensing performance to previously reported studies of various sensing electrodes.

Sensing electrodes	Sensitivity Pb (II)/($\mu\text{A ppb}^{-1}$)	Ref.
Bi/EPPGE	0.0354	[16]
Unmodified EPPGE	0.954	[17]
Bi nanopowder/SPE	0.715	[18]
Bi/MWCNTs; Nafion/GCE	0.218; 0.271	[19]
Bi/ABTS-MWCNTs/GCE	0.532	[20]
Bi/CNTs/PSS/GCE	0.0792	[21]
Bi/Graphene-Nafion	0.950	[22]
MWCNTs	0.101	[23]
Hg film/SPEs	0.085	[24]
Heated graphite nanoparticle-based SPEs	0.014	[25]
MgO nanoflowers	3.410	[26]
Fe ₃ O ₄	0.049	[27]
rGO-Fe ₃ O ₄	0.066	[28]
rGO-Fe ₃ O ₄ nano composites	0.092	[29]
MgO-nafion GCE	0.026	[30]
Layered Co ₃ O ₄ /nafion GCE	0.136	[31]
poMWCNTs GCE	0.017	[32]
MnO ₂ nanoparticles GCE	0.021	[33]
Nanoplate-stacked Fe ₃ O ₄ GCE	0.119	[34]
MgSiO ₃ /nafion GCE	0.046	[35]
MnFe ₂ O ₄ GCE	0.096	[36]
MnFe ₂ O ₄ @Cys GCE	0.275	[37]
MgFe-LDH/graphene/GCE	0.276	[38]
[Ru(bpy) ₃] ²⁺ -GO	0.116	[39]
Co:ZnO/RGO/GCE	0.117	[40]
L-cys-rGO/GCE	0.023	[41]
MnFe ₂ O ₄ /GO/GCE	0.164	[42]
AgNPs/RGO/GCE	0.235	[43]
NH ₂ -MIL-88(Fe)-rGO/GCE	0.164	[44]
MoS ₂ /rGO/GCE	0.241	[45]
Exp 1/GPE	1.979	This study
Exp 2/GPE	1.962	This study
Exp 3/GPE	2.170	This study
Exp 4/GPE	2.710	This study

Notes: MWCNTs, multi-walled carbon nanotubes; PSS, poly(sodium 4-styrenesulfonate); ABTS, 2,2'-azinobis(3-ethylbenzothiazoline-6-sulfonate) diammonium salt; EPPGE, edge plane pyrolytic graphite electrode; SPEs, screen-printed electrodes; GCE, glass carbon electrode; LOD, limit of detection; MgFe-LDH, hierarchical MgFe-layered double hydroxide; [Ru(bpy)₃]²⁺-GO, ruthenium(II) bipyridine complex-graphene oxide; Co:ZnO, cobalt doped ZnO; G, graphene; IAP30/RTIL, irradiated attapulgite at a fluence of 30 kGy with room temperature ionic liquid.

exhibits a weight loss of 17.38% may be due to the removal of residual monomers and trapped water molecules. The second stage from 400 to 900 °C, this decomposition is characterized by a weight loss of 62.33% due to short chain fragments created by chain scission.

The thermogram of exp (4) showed two stages of thermal decomposition. The first stage from room temperature to 400 °C with a maximum at 250 °C exhibits a weight loss of 18.93% may be due to the removal of residual monomers and trapped water

molecules. The second stage from 400 to 900 °C, this decomposition is characterized by a weight loss of 75.99% due to short chain fragments created by chain scission.

The thermal characterization shows clearly that existence of ligand in the template polymer enhance the thermal stability of group (1) polymers compared with polymers of group (2) due to the big difference observed in the weight loss results.

3.3. Electrochemical analysis

3.3.1. Optimum experimental pH condition

The first step of the experiment is to test the sensing performance of working electrodes toward Pb (II). The effect of solution pH in citric/phosphate as buffer in the following discussion demonstrated this case. With various working electrodes, the cyclic voltammograms were recorded as shown in Fig. 10. Figure 10 shows the cyclic voltammograms of 50 ppb Pb (II) using four different electrodes to get well-defined, more sensitive signals and obtain the best response for electrochemical detection of lead metal ions with the experiments of group (1)/GPE modified electrodes and group (2)/GPE modified electrodes. The best pH of the working buffer solution for CV measurements was selected by the criteria of high and sharp current signal at pH 4.6.

3.3.2. Electrochemical response of modified electrodes for determination of Pb (II)

The individual measurements of Pb (II) using modified GPE electrodes were performed as shown in Fig. 11. Figure 11a–11d shows the square wave voltammetry (SWV) responses of the modified GPE electrodes for Pb (II) at different concentrations, and the corresponding calibration curves being derived accordingly (inset in Fig. 11a–d). At potentials of approximately 0.5 V, Pb (II) is detected, Peak current varies from 1.5 to 9.5 ppb in direct proportion to Pb (II) concentration. For all following analyses, a pulse amplitude of 25 mV was applied.

The regression equation is as follows,

$$I_p = a + bC$$

where I_p is the peak current (μA); C is the concentration of metal ion (ppb); a , b is intercept and slope, respectively. The sensitivity of sensors (b) to Pb (II), intercepts (a), and correlation coefficients related to four modified electrodes were listed in Table 5.

To illustrate the effectiveness of the proposed modified electrodes, The determination of Pb (II) ions using these modified electrodes was compared with previously reported various electrodes. It was

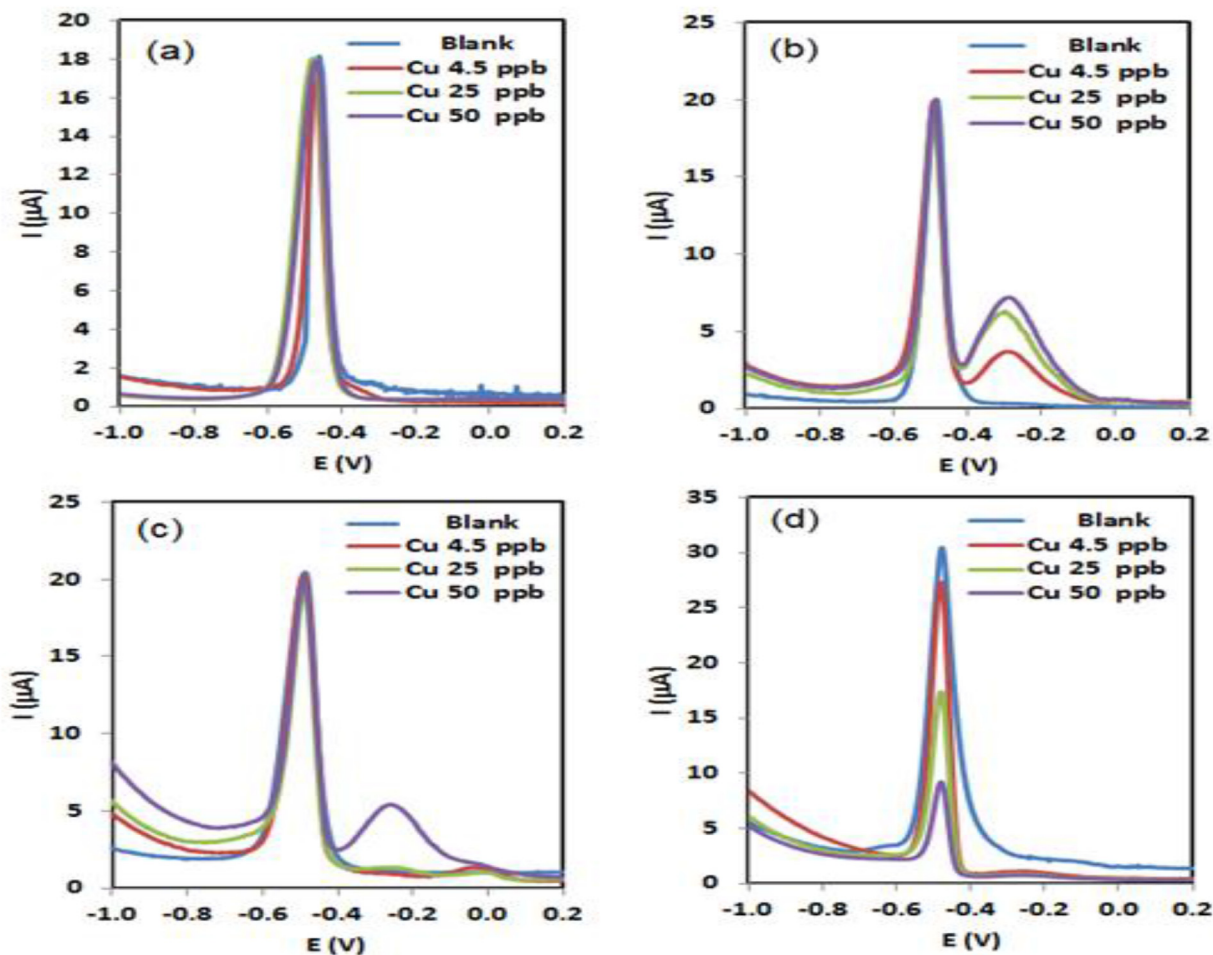


Fig. 12. Interference of Cu (II) metal ions on the stripping peak currents of the exp 1/GPE (a), exp 2/GPE (b), exp 3/GPE (c), exp 4/GPE (d), for the individual analysis of Pb (II) ions.

found that these electrodes have more sensitivity toward Pb (II) than the majority of other Bi-based electrodes for the detection of Pb (II). The comprehensive comparison with previously reported studies is summarized in Table 6.

3.3.3. Interference and selectivity studies

After completing the individual of Pb (II), we will study the mutual interferences of Pb (II) with Cu (II), or Fe (III) at the GPE-modified electrodes.

The interference was studied by calculating the percentage of peak current of the competing ions to the peak current of the individual lead ions as the follow:

$$\text{Interference \%} = \left[1 - \frac{I_{int}}{I_{Pb}} \right] 100$$

where I_{Pb} , I_{int} are peak currents for lead and interfere ion respectively.

When fixing the concentration at 9.5 ppb of Pb (II), with increasing Cu (II) ion concentrations 4.5, 25, and 50 ppb, the signals were found to be no change was noted for Pb (II) at various concentrations of Cu (II) ion when utilize exp 1, exp 2, or exp 3 modified electrodes (Fig. 12).

While it was noted that there was a difference in the values of the peak current when the concentration of copper ions changed using exp 4 modified electrode, and it was clear from this that the presence of copper ions affected the determination of the concentration of lead ions if they were found with them in the same solution. Similar results could be obtained when fixing the concentration of Pb (II) at 9.5 ppb variation of Fe (III) ion concentrations 4.5, 25, and 50 ppb (Fig. 13).

The calculated interference percentages were around zero, this reinforces the impression that these values are very close to that for individual measurement of Pb (II), and relative standard deviation (RSD %) value was less than 10%, as shown in Table 7.

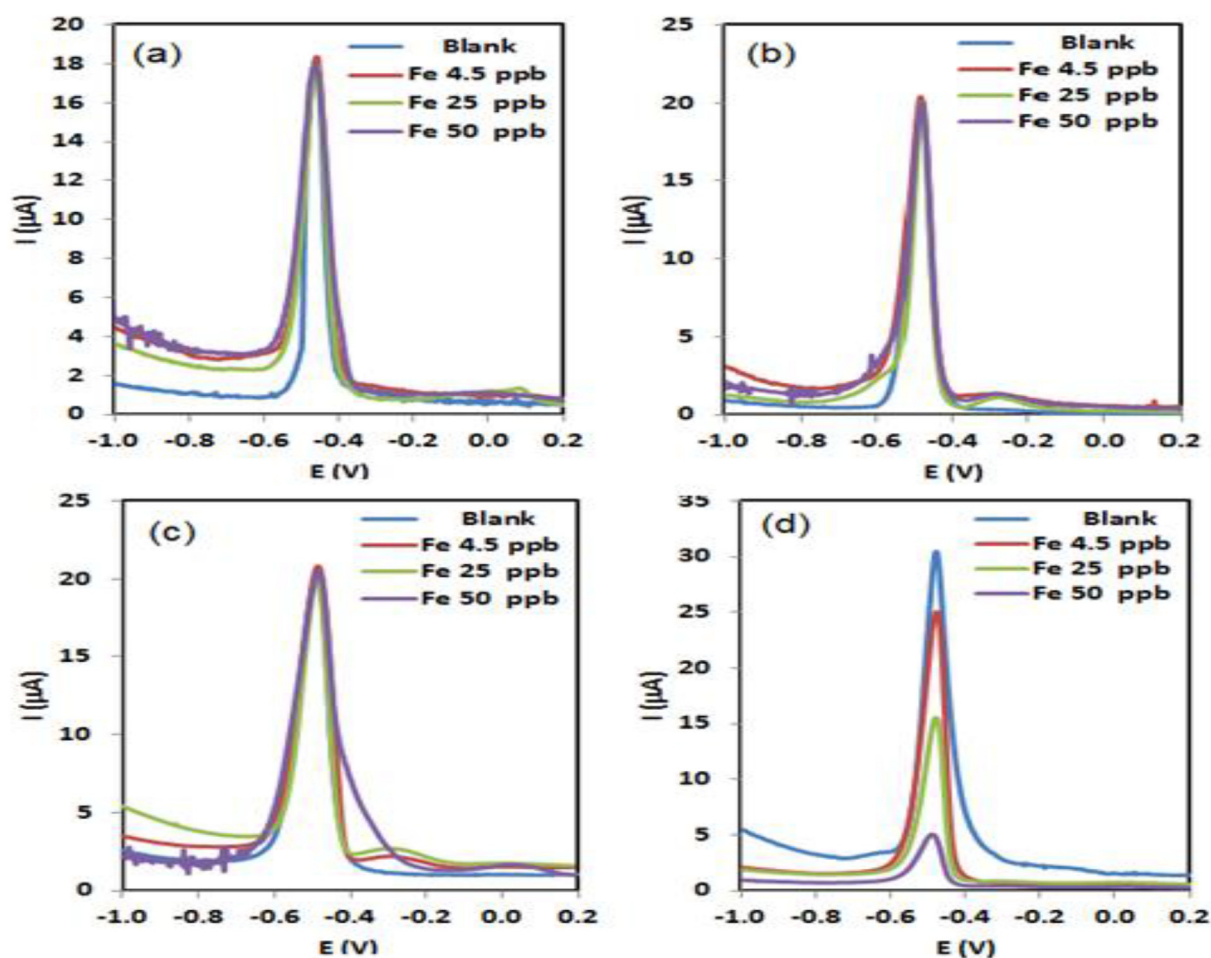


Fig. 13. Interference of Fe (III) metal ions on the stripping peak currents of the exp 1/GPE (a), exp 2/GPE (b), exp 3/GPE (c), exp 4/GPE (d), for the individual analysis of Pb (II) ions.

Table 7. Interference percentage and relative standard deviation using modified electrodes.

Modified Electrode	Interfere metal ions (ppb)	Interfere (%)	RSD %	
Exp 1/GPE	Fe (III)	4.5	-1.3	3.9
		25	0.8	
		50	0.8	
	Cu (II)	4.5	1.0	2.1
		25	0.6	
		50	1.2	
Exp 2/GPE	Fe (III)	4.5	-1.8	3.7
		25	-0.2	
		50	0.0	
	Cu (II)	4.5	0.6	8.2
		25	4.3	
		50	1.3	
Exp 3/GPE	Fe (III)	4.5	-1.7	7.4
		25	2.3	
		50	0.0	
	Cu (II)	4.5	0.8	11.1
		25	5.7	
		50	2.5	
Exp 4/GPE	Fe (III)	4.5	19.5	247.7
		25	50.7	
		50	85.9	
	Cu (II)	4.5	10.4	209.6
		25	42.9	
		50	69.8	

4. Conclusion

From observed data of the thermal analysis of both group (1) and group (2) we can conclude that group (1) is more thermal stable than group (2) that can be explained by the presence of ligand in polymers of group (1) improve the thermal stability than its absence.

We conclude from this study, all the electrochemical analysis indicates that the selectivity of Pb (II) on exp (3), exp (1), exp (2) modified electrodes is unaffected by the presence of Cu (II) or Fe (III) ions.

Conflicts of interest

Authors declare that there is no conflict of interest.

Acknowledgements

The authors extend their sincere thanks and appreciation to the Department of Chemistry, Faculty of Science, Al-Azhar University for their endless support for researchers and scientific research with all its requirements.

References

- [1] Wu Y, Lin S, Tian H, Zhang K, Wang Y, Sun B, et al. A quantitative assessment of atmospheric emissions and spatial distribution of trace elements from natural sources in China. *Environ Pollut* 2020;259:113918.
- [2] Lu Y, Liang X, Niyungeko C, Zhou J, Xu J, Tian G. A review of the identification and detection of heavy metal ions in the environment by voltammetry. *Talanta* 2018;178:324–38.
- [3] Marton M, Michniak P, Behul M, Rehacek V, Stanova AV, Redhammer R, et al. Bismuth modified boron doped diamond electrode for simultaneous determination of Zn, Cd and Pb ions by square wave anodic stripping voltammetry: influence of boron concentration and surface morphology. *Vacuum* 2019;167:182–8.
- [4] Thanh NM, Van Hop N, Luyen ND, Phong NH, Tam Toan TT. Simultaneous determination of Zn (II), Cd (II), Pb (II), and Cu (II) using differential pulse anodic stripping voltammetry at a bismuth film-modified electrode. *Adv Mater Sci Eng* 2019;2019.
- [5] Maldonado VY, Espinoza-Montero PJ, Rusinek CA, Swain GM. Analysis of Ag (I) biocide in water samples using anodic stripping voltammetry with a boron-doped diamond disk electrode. *Anal Chem* 2018;90:6477–85.
- [6] Zhao G, Tong X, Hu Z, Xiao X, Li D. Electrochemical costripping models and mutual interferences of multi-transition metal systems on the surface of boron-doped diamond. *Electrochim Acta* 2008;53:4283–92.
- [7] Ferreira R, Chaar J, Baldan M, Braga N. Simultaneous voltammetric detection of Fe³⁺, Cu²⁺, Zn²⁺, Pb²⁺ + e Cd²⁺ in fuel ethanol using anodic stripping voltammetry and boron-doped diamond electrodes. *Fuel* 2021;291:120104.
- [8] Zhai Z, Huang N, Zhuang H, Liu L, Yang B, Wang C, et al. A diamond/graphite nanoplatelets electrode for anodic stripping voltammetric trace determination of Zn (II), Cd (II), Pb (II) and Cu (II). *Appl Surf Sci* 2018;457:1192–201.
- [9] Sylvestre KK, Ollo K, Etienne KK, Jocelin KK, Lassiné O. Detection of lead (II) on a boron-doped diamond electrode by differential pulse anodic stripping voltammetry. *Chem Sci Int J* 2021;30(7):33–46.
- [10] Ninwong B, Ratnarathorn N, Henry CS, Mace CR, Dungchai W. Dual sample preconcentration for simultaneous quantification of metal ions using electrochemical and colorimetric assays. *ACS Sens* 2020;5:3999–4008.
- [11] Khadro B, Sikora A, Loir AS, Errachid A, Garrelie F, Donnet C, et al. Electrochemical performances of B doped and undoped diamond-like carbon (DLC) films deposited by femtosecond pulsed laser ablation for heavy metal detection using square wave anodic stripping voltammetry (SWASV) technique. *Sensor Actuator B Chem* 2011;155:120–5.
- [12] Hasanah AN, Safitri N, Zulfa A, Neli N, Rahayu D. Factors affecting preparation of molecularly imprinted polymer and methods on finding template-monomer interaction as the key of selective properties of the materials. *Molecules* 2021; 26:5612.
- [13] Deng F, Luo XB, Ding L, Luo SL. Application of nanomaterials and nanotechnology in the reutilization of metal ion from wastewater. In: *Nanomaterials for the removal of pollutants and resource reutilization*. Elsevier; 2019 Jan 1. p. 149–78.
- [14] Fereidoonipour F, Rajabi HR. Development of flow injection analysis-solid phase extraction based on ion imprinted polymeric nanoparticles as an efficient and selective technique for preconcentration of zinc ions from aqueous solution. *New J Chem* 2017;41:8828–36.
- [15] Ventura S, Bhamidi S, Hornbostel M. Selective recovery of lithium from brines. In: *43rd workshop on geothermal reservoir engineering*. Stanford University; 2018 Feb.
- [16] Kachooosangi RT, Banks CE, Ji X, Compton RG. Electroanalytical determination of cadmium (II) and lead (II) using an in-situ bismuth film modified edge plane pyrolytic graphite electrode. *Anal Sci* 2007;23:283–9.
- [17] Lu M, Toghiani KE, Compton RG. Simultaneous detection of trace cadmium (II) and lead (II) using an unmodified edge plane pyrolytic graphite electrode. *Electroanalysis* 2011;23: 1089–94.
- [18] Lee GJ, Lee HM, Rhee CK. Bismuth nano-powder electrode for trace analysis of heavy metals using anodic stripping voltammetry. *Electrochem Commun* 2007;9:2514–8.
- [19] Xu H, Zeng L, Xing S, Xian Y, Shi G, Jin L. Ultrasensitive voltammetric detection of trace lead (II) and cadmium (II) using MWCNTs-nafion/bismuth composite electrodes. *Electroanalysis: Int J Dev Fund Pract Aspect Electroanal* 2008;20:2655–62.
- [20] Deng W, Tan Y, Fang Z, Xie Q, Li Y, Liang X, et al. ABTS-Multiwalled carbon nanotubes nanocomposite/Bi film electrode for sensitive determination of Cd and Pb by differential pulse stripping voltammetry. *Electroanalysis: Int J Dev Fund Pract Aspect Electroanal* 2009;21:2477–85.
- [21] Jia X, Li J, Wang E. High-sensitivity determination of lead (II) and cadmium (II) based on the CNTs-PSS/Bi composite film electrode. *Electroanalysis* 2010;22:1682–7.
- [22] Li J, Guo S, Zhai Y, Wang E. High-sensitivity determination of lead and cadmium based on the Nafion-graphene composite film. *Anal Chim Acta* 2009;649:196–201.
- [23] Wu K, Hu S, Fei J, Bai W. Mercury-free simultaneous determination of cadmium and lead at a glassy carbon electrode modified with multi-wall carbon nanotubes. *Anal Chim Acta* 2003;489:215–21.
- [24] Güell R, Aragay G, Fontàs C, Anticó E, Merkoçi A. Sensitive and stable monitoring of lead and cadmium in seawater using screen-printed electrode and electrochemical stripping analysis. *Anal Chim Acta* 2008;627:219–24.
- [25] Aragay G, Pons J, Merkoçi A. Enhanced electrochemical detection of heavy metals at heated graphite nanoparticle-based screen-printed electrodes. *J Mater Chem* 2011;21: 4326–31.
- [26] Wei Y, Yang R, Yu XY, Wang L, Liu JH, Huang XJ. Stripping voltammetry study of ultra-trace toxic metal ions on highly selectively adsorptive porous magnesium oxide nanoflowers. *Analyst* 2012;137:2183–91.
- [27] Xiong S, Wang M, Cai D, Li Y, Gu N, Wu Z. Electrochemical detection of Pb (II) by glassy carbon electrode modified with amine-functionalized magnetite nanoparticles. *Anal Lett* 2013;46:912–22.
- [28] Sun Y, Zhang W, Yu H, Hou C, Li DS, Zhang Y, et al. Controlled synthesis various shapes Fe₃O₄ decorated reduced graphene oxide applied in the electrochemical detection. *J Alloys Compd* 2015;638:182–7.
- [29] Xiong S, Yang B, Cai D, Qiu G, Wu Z. Individual and simultaneous stripping voltammetric and mutual interference analysis of Cd²⁺, Pb²⁺ and Hg²⁺ with reduced graphene oxide-Fe₃O₄ nanocomposites. *Electrochim Acta* 2015; 185:52–61.
- [30] Wu Z, Xu C, Chen H, Wu Y, Yu H, Ye Y, et al. Mesoporous MgO nanosheets: 1, 6-hexanediamine-assisted synthesis and their applications on electrochemical detection of toxic metal ions. *J Phys Chem Solid* 2013;74:1032–8.
- [31] Liu ZG, Chen X, Liu JH, Huang XJ. Well-arranged porous Co₃O₄ microspheres for electrochemistry of Pb (II) revealed by stripping voltammetry. *Electrochem Commun* 2013;30: 59–62.
- [32] Wei Y, Liu ZG, Yu XY, Wang L, Liu JH, Huang XJ. O₂-plasma oxidized multi-walled carbon nanotubes for Cd (II) and Pb (II) detection: evidence of adsorption capacity for electrochemical sensing. *Electrochem Commun* 2011;13:1506–9.
- [33] Zhang QX, Peng D, Huang XJ. Effect of morphology of α -MnO₂ nanocrystals on electrochemical detection of toxic metal ions. *Electrochem Commun* 2013;34:270–3.
- [34] Li WJ, Yao XZ, Guo Z, Liu JH, Huang XJ. Fe₃O₄ with novel nanoplate-stacked structure: surfactant-free hydrothermal synthesis and application in detection of heavy metal ions. *J Electroanal Chem* 2015;749:75–82.
- [35] Xu RX, Yu XY, Gao C, Jiang YJ, Han DD, Liu JH, et al. Non-conductive nanomaterial enhanced electrochemical response in stripping voltammetry: the use of nanostructured

- magnesium silicate hollow spheres for heavy metal ions detection. *Anal Chim Acta* 2013;790:31–8.
- [36] Liu ZG, Chen X, Liu JH, Huang XJ. Robust electrochemical analysis of as (III) integrating with interference tests: a case study in groundwater. *J Hazard Mater* 2014;278:66–74.
- [37] Zhou SF, Wang JJ, Gan L, Han XJ, Fan HL, Mei LY, et al. Individual and simultaneous electrochemical detection toward heavy metal ions based on L-cysteine modified mesoporous MnFe₂O₄ nanocrystal clusters. *J Alloys Compd* 2017;721:492–500.
- [38] Ma Y, Wang Y, Xie D, Gu Y, Zhu X, Zhang H, et al. Hierarchical MgFe-layered double hydroxide microsphere/graphene composite for simultaneous electrochemical determination of trace Pb (II) and Cd (II). *Chem Eng J* 2018;347:953–62.
- [39] Gumpu MB, Veerapandian M, Krishnan UM, Rayappan JB. Simultaneous electrochemical detection of Cd (II), Pb (II), as (III) and Hg (II) ions using ruthenium (II)-textured graphene oxide nanocomposite. *Talanta* 2017;162:574–82.
- [40] Karthik R, Thambidurai S. Synthesis of cobalt doped ZnO/reduced graphene oxide nanorods as active material for heavy metal ions sensor and antibacterial activity. *J Alloys Compd* 2017;715:254–65.
- [41] Muralikrishna S, Sureshkumar K, Varley TS, Nagaraju DH, Ramakrishnappa T. In situ reduction and functionalization of graphene oxide with L-cysteine for simultaneous electrochemical determination of cadmium (II), lead (II), copper (II), and mercury (II) ions. *Anal Methods* 2014;6:8698–705.
- [42] Zhou SF, Han XJ, Fan HL, Huang J, Liu YQ. Enhanced electrochemical performance for sensing Pb (II) based on graphene oxide incorporated mesoporous MnFe₂O₄ nanocomposites. *J Alloys Compd* 2018;747:447–54.
- [43] Sang S, Li D, Zhang H, Sun Y, Jian A, Zhang Q, et al. Facile synthesis of AgNPs on reduced graphene oxide for highly sensitive simultaneous detection of heavy metal ions. *RSC Adv* 2017;7:21618–24.
- [44] Duan S, Huang Y. Electrochemical sensor using NH₂-MIL-88 (Fe)-rGO composite for trace Cd²⁺, Pb²⁺, and Cu²⁺ detection. *J Electroanal Chem* 2017;807:253–60.
- [45] Sun YF, Sun JH, Wang J, Pi ZX, Wang LC, Yang M, et al. Sensitive and anti-interference stripping voltammetry analysis of Pb (II) in water using flower-like MoS₂/rGO composite with ultra-thin nanosheets. *Anal Chim Acta* 2019;1063:64–74.